British Journal of Applied Science & Technology
3(4): 1430-1446, 2013

SCIENCEDOMAIN *international*
www.sciencedomain.org

ANSYS Simulation of Loads Experienced by the Peduncle of a Design of Robotic Fish

M. O. Afolayan[1*], D. S. Yawas[1], C. O. Folayan[1] and S. Y. Aku[1]

[1]Mechanical Engineering Department, Ahmadu Bello University, Zaria, Nigeria.

Authors' contributions

This work was carried out in collaboration between all the authors. Author MOA designed the study, and wrote the first draft of the manuscript. Authors DSY, COF and SYA supervised the project, read through it and ensure accuracy of all the information reported.

Research Article

Received 19th June 2013
Accepted 21st August 2013
Published 23rd September 2013

ABSTRACT

Aims: This article aims at simulating the forces and dynamic load that the peduncle of a robotic fish using vulcanized natural rubber for its joint and plywood for its tail fin will experience.
Methodology: Using standard strength of material equations and constitutive equation that fits the selected natural rubber, the loads that will be encountered in a water with density 990kg/m^3 were calculated. The result was then used in ANSYS multiphysics environment to setup the simulation of the response of the peduncle to the calculated loads. Autodesk Inventor 7 was used for the geometrical drawings and calculations such as area and centroid of the non standard shape. Furthermore, the Payne effect for the rubber joint was found experimentally as its result will guide in the threshold of tail oscillation frequency allowed.
Results: von Mises stress within the components of the peduncle due to the drag load was found to be 0.03kN/m^2 to 4.64kN/m^2 for the rubber and 0.03kN/m^2 to 41.48kN/m^2 for the plywood fin. Stress experienced by the peduncle under its own weight shows that for the rubber component, the maximum von Mises stress experienced by the rubber is 4.9kN/m^2 and for the plywood material, it is 1.087kN/m^2. Test for warping/ bending of the peduncle shows a straight isoline pattern. Tensile stress within the epoxy bonded joints shows a uniform bond pattern. The dynamic torque experienced by the peduncle increases with frequency of oscillation and even more rapidly as the angle of swing increases though at a fixed ratio to each other. Frequency induced softening (Payne effect) shows that the rubber will become soft as the frequency reaches 25Hz.

**Corresponding author: E-mail: tunde_afolayan@yahoo.com;*

Conclusion: The use of plywood material for the fin and vulcanized natural rubber for the joint and using epoxy glue for the designed peduncle of the robotic fish will be capable of withstanding the stresses that will be developed in real life scenario.

Keywords: ANSYS; robotic fish; biomimetic; hyper-redundant; simulation; peduncle.

1. INTRODUCTION

According to Lilianes [1], biomimetic robots, evolutionary robots, emotion controlled robots are ideas imitating life with different approach. Several functional biologically inspired robots are already in service [2] such as Sony AIBO, Honda ASIMO, Toyota Flute playing robot, Wall gecko (wall climbing robot) from Stanford University and lately DARPA humming bird robot. Biomimetic robots imitate some characteristics of life forms such as mobility [3], vision [3-7], flying [3,7,8] and navigational methodology. Biomimetic systems are greatly desired because natural systems are highly optimized and efficient. Srinivasan [6] calls them shortcuts to mathematically complex issues of life. Take a look at fly or honey bee, they have very small brain and processing power, no researcher has ever built a robot with such visual capabilities like them at such a scale at least to our knowledge. Nearly all the five senses of living being i.e. sight or vision [3,7], hearing and touch [9,10], smell [11] and taste [12] are imitated. The semi-autonomous indoor airplane by [3] was possible because of its mimicry of insect vision using optical flow.

A robotic fish as a form of Hyper-redundant robots [13] has its own merits; such as ability to function after losing mobility in one or more sections, stability on all terrain because of low center of gravity, terrainability which is the ability to traverse rough terrain, small size that can penetrate small crevices and are capable of being amphibious by sealing the whole body, the same body motion on land is then used for swimming in water as exemplified by ACM-R5 robot [14,15]. Hyper-redundant robot have their own limitations also, such as low speed as the whole body is used for motion, [16], poor thermal control because of low surface to volume ratio, [17] and how to control, programme and build an efficient control system for the several degrees of freedom (DOF) links or joints they are made up of.

The main organ of proportion for teleost species of fish like mackerel (being the focus of this work) is its tail fin and the joint between it and the body as shown in Fig. 1(A). This whole structure is referred to as the peduncle. Building a biomimetic robot in the form of teleost species of fish implies that careful attention should be paid to the peduncle design and the material selected to get a successful performance. Also, the angle of bending varies on either side which brings about heavy load (tensile and compressive loading) on the joint especially. This joint must be able to withstand whatever load it will encounter in service.

A solution to this problem is to use a carbon-filled natural rubber for the joint and a rigid but thin plywood material for the fin as shown in Fig. 1(B). The rubber can take up very large number of oscillation and the plywood is expected to take up the drag load due to the paddling action of the tail motion. Rubber is selected because it is qualitatively similar to biological materials (such as muscles) in its stress-stretch behavior [18].

The question that comes to mind is that, what is the load pattern the main organ of proportion is experiencing? Will the design work? Will the rubber joint collapse? Will the thin plywood work also? What type of loading is the rubber-epoxy-plywood interface

experiencing? To answer these questions, computer simulation was deemed to be the next logical steps. A simulation procedure will be able to predict if the design will work or not.

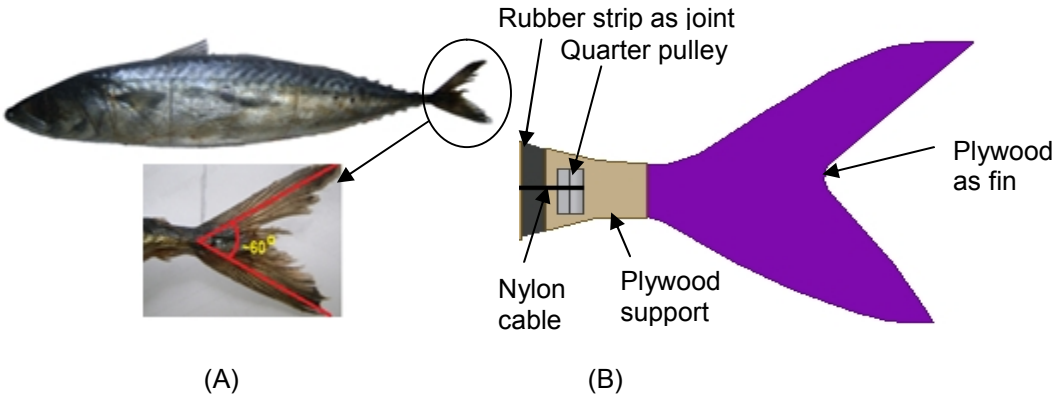

Fig. 1. The peduncle of a dead 394mm mackerel fish (A) and a drawing of the peduncle (B)

This article scope is limited to application of ANSYS multiphysics software to simulate the designed peduncle responses to applied loads. In addition, a section will be dedicated to the rubber dynamic behavior as its behavior is core to the success of the peduncle design.

This work is justified because;

1. teleost species of fish have the highest acceleration and swimming speed [19] that is worth imitating in underwater robotics.
2. the peduncle has the thinnest section (hence the limiting factor) of the whole fish structure.
3. robotic fish in the form of teleost fishes can transform the way we build underwater robots and unmanned vehicles, because fishes swimming modes creates less wakes and can be camouflaged for stealth operation and as decoy for catching preys.
4. use of rubber for the peduncle helps simplifies the control strategy involved in hyper-redundant robot design. Most researchers have been extrapolating convectional joints – hinge, universal, even ball and sockets in an attempt to build hyper-redundant robot. These approaches have made many of those robots unsuccessful in their imitation of nature [20].

2. MATERIALS AND METHODS

From the drawing of Fig. 1B, the peduncle of the robotic fish is made up of 1.5mm thick vulcanized natural rubber joint and 1/8 inch (3.2mm) thick seasoned plywood fin. These two materials are held together with epoxy glue. The fin motion (Fig. 2) is controlled by a taut nylon cable that is passed over quarter pulleys (5mm radius) and connected to a servo motor which under the control of a microcontroller, impact a defined oscillatory motion pattern to it.

To simulate the loads, a finite element tool, ANSYS Multiphysis version 10 was selected and for all the geometry work, Autodesk Inventor 7 was used.

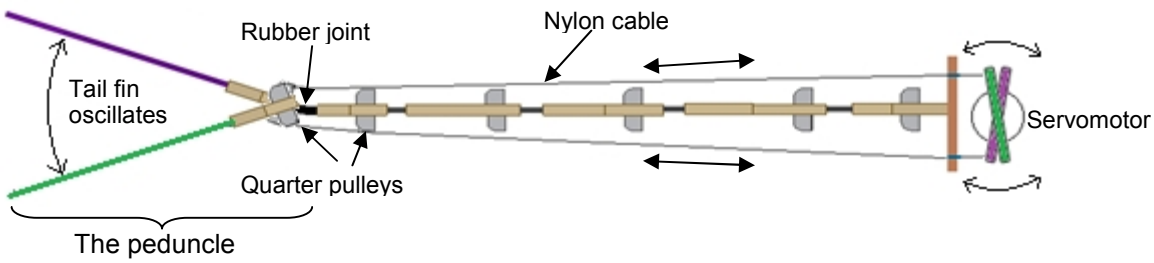

Fig. 2. The robot tail cable controlled design

From this particular robotic tail fish design, the major active components to bring about the peduncle motion for swimming to take place are the tail fin, the rubber joint, the nylon cable and the servomotor.

2.1 Simulation Procedures/Steps

2.1.1 Theoretical backgrounds

1. Stresses within an elastomer (rubber) are determined using finite strain elasticity theory or constitutive equations because it has unique properties; in particular, it has exceptionally low shear modulus and high elastic strain capability.

2. The plywood is treated as a linear material and the following mechanical properties were used in its finite element analysis [21,22];

   a. Stress $$\sigma = \frac{Load}{Area} \quad (1)$$

   b. Strain $$\epsilon = \frac{Change\ in\ length}{Original\ length} \quad (2)$$

   c. Modulus of elasticity or Young's modulus; $$E = \frac{Stress}{Strain} \quad (3)$$

   d. Poisson's ratio $$v = \frac{Lateral\ strain}{Longitudinal\ strain} \quad (4)$$

   e. Density, (5)

   f. Yield strength (von Mises stress) $$\sigma_v = \sqrt{\frac{(\sigma_1-\sigma_2)^2+(\sigma_2-\sigma_3)^2+(\sigma_1-\sigma_3)^2}{2}} \quad (6)$$

   where σ_1, σ_2 and σ_3 are the principal stresses

3. Forces experienced by a moving foil (or plate) inside water: When the fish tail oscillates inside the water, it behaves like a plate. The main force acting on the plate with area **A** is the drag force, F_d. [23] given as

$$F_d = \frac{1}{2}\rho v^2 C_d A \quad (7)$$

where ρ = density of fluid (water in this case)
C_d = coefficient of drag. It is shape dependent, in this work, it is assumed to be perfectly flat.
A = Area of plate
v = velocity of the plate (peduncle)

4. Stress in the nylon cable is assumed linear and follows Hooke's law.
5. Tensile stress within the glue is assumed to follow mechanical interlocking theory which is based on the fact that at the microscopic level all surfaces are very rough and consist of crevices, cracks and pores. The adhesive penetrates these features and hardens such that it keys into the surfaces and forms a strong surface bond [24]. The stress is given as

$$\sigma_g = \frac{P_g}{A_g} \quad (8)$$

where P_g= separating forces acting on the glued bodies
A_g= area of glue

6. The dynamic pressure, P_v caused by the tail pushing water at velocity angular ω is given by Bernoulli's equation of the form

$$P_v = 0.5\ \rho\ \omega_v^2 \quad (N\ m^{-2}), \quad [24] \quad (9)$$

where P_v = dynamic pressure
ρ = water density
ω_v = angular velocity of the fish tail

This dynamic pressure was derived using large-amplitude elongated-body motion theory by Lighthill [25] which allowed the prediction of instantaneous reactive force between fish and water for fish motions of arbitrary amplitude. Fig. 3 shows the force components and velocity components of a fish peduncle as well as the torque and angular velocity experienced by it. The force F_v is zero (F_v=0 N) for a fish that is stationary or coasting; also ω=0. Coasting arises when a fish stops wagging its tail and just glides along its path in a straight manner. Force F_v is non zero when there is tail motion.

Thus we have (with equation 9)

$$F_v = \begin{cases} 0 & coasting \\ 0.5\rho\omega_v^2 & swimming \end{cases} \quad (10)$$

From which the dynamic torque T, is calculated.

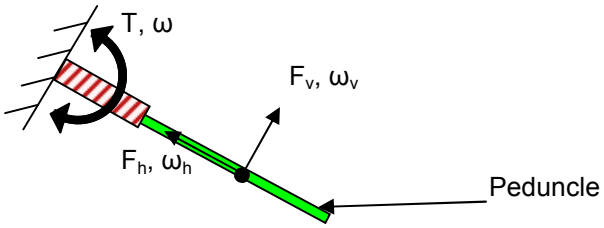

Fig. 3. Instantaneous force and velocity component of an active tail fin. Horizontal velocity component ωh is assumed negligible - disturbance to water along that axis is small [23]

7. Mullins effect: Preconditioning rubber material by uniaxial loading and unloading is known as stress-softening and is referred to as Mullins effect. Stress-softening of elastomer is an incompressible, isotropic and nonlinear behaviour whose mechanical response depends on its deformation history – [20]. Mullins materials have a selective memory of only previous maximum strain experienced during its deformation history but not how it got there. The magnitude of strain *m* is defined as

$$m \equiv \|\mathbf{B}\| = \sqrt{\mathbf{B}.\mathbf{B}} \quad \text{, [26]} \tag{11}$$

in terms of the left Cauchy-Green deformation tensor $\mathbf{B} \equiv \mathbf{F}\mathbf{F}^{\mathbf{T}}$.

F is the deformation and in the undistorted state for which **B** = 1, we have $m=\sqrt{3}$; otherwise, $m>\sqrt{3}$ for all isochoric deformations. For a virgin material, the maximum previous strain is the current value of *m*. When the material is stretched, the magnitude of strain value changes to $M=m_{max}$ it experienced. As long as any subsequent stretching does not pass this *M*, it retraces its steps / pattern when stretched again.

8. Payne effect – frequency induced softening: A membrane with mass density of ρ will have fundamental/ natural frequency v as

$$v = \gamma\sqrt{\frac{T}{\rho A}} \quad , \tag{12}$$

where T = the tension within the elastomer
ρ = mass density
A = Area of elastomer
γ= a dimensionless constant

For a virgin material the frequency can be written as

$$v = v(T,\lambda) = \nu_0\sqrt{\frac{T}{\mu_{0\lambda^2}}} \quad \text{,[26]} \tag{13}$$

where λ = the isochoric equibaxial stretch
μ_o = shear modulus of the material in its undisturbed state
$v_o = \gamma\sqrt{t_0\mu_0/\rho_0 A_0}$
t_0 = current elastomer thickness
ρ_0 = current density

A_0 = current area of elastomer

For a stress-softened material, the frequency is

$$v_s = v(\tau,\lambda) = \nu_0 \sqrt{\frac{\tau}{\mu_0 \lambda^2}} \quad ,[26] \tag{14}$$

where τ = the stress within the softened material

$$T \geq \tau \quad , \tag{15}$$

$$\text{therefore} \quad \frac{v}{v_s} = \sqrt{\frac{T}{\tau}} \geq 1 \quad , \tag{16}$$

which implies that the vibration frequency of the virgin material is greater than the corresponding frequency of the stress-softened material for each fixed stretch value.

2.1.2 The simulation parameters/constraints

The following steps were taken in setting up the finite element tool;

1. Input of material physical data
2. Selecting the constitutive equation to use for the rubber
3. Design of mesh element,
4. Determination of the simulated loads,

a) Specification of the material physical data

The following data was used as the physical property of the plywood material:

Young's modulus	$5x10^9$ Pa
Poisson's ratio	0.25
Density	$500kg/m^3$
Tensile yield strength	$1.5x10^7$ Pa
Compressive yield strength	$3.6\ x10^7$ Pa
Tensile ultimate strength	$3.1\ x10^7$ Pa
Compressive ultimate strength	$2.0\ x10^7$ Pa

For the rubber material: the inputs are uniaxial and biaxial test data shown graphically in Fig. 4. The lines are the ANSYS prediction of the material behaviour, while the smooth lines are the inputs data (uniaxial and biaxial) from experimental measurements.

b) Selecting constitutive equation

Determining which constitutive equation will best predict the behaviour of the particular sample rubber being tested require curve fiting using the tools provided in the ANSYS Multiphysis version 10. The tool indicates that Mooney–Rivlin parameter (equation 17) constitituve equation is adequate to predict the behaviour of the rubber sample from Fig. 4.

$$W = c_{10}(\bar{I}_1 - 3) + c_{01}(\bar{I}_2 - 3) + c_{20}(\bar{I}_1 - 3)^2 + c_{11}(\bar{I}_1 - 3)(\bar{I}_2 - 3) + c_{02}(\bar{I}_2 - 3)^2 + c_{30}(\bar{I}_2 - 3)^3 + c_{21}(\bar{I}_1 - 3)^2(\bar{I}_2 - 3) + c_{12}(\bar{I}_1 - 3)(\bar{I}_2 - 3)^2 + c_{03}(\bar{I}_2 - 3)^3 + \frac{1}{d}(J - 1)^2 \quad (17)$$

where W = strain energy
J = determinant of the elastic deformation gradient F
$\bar{I}_1$= first deviatoric strain invariant
$\bar{I}_2$= second deviatoric strain invariant
c_{10}, c_{01} = material constants characterizing the deviatoric deformation of the material
d = material incompressibility parameter

The initial shear modulus is defined as:

$\mu = 2(c_{10} + c_{01})$

and the initial bulk modulus is defined as:

$K = 2/d$ where $d=(1-2*\nu)/(c_{10} + c_{01})$

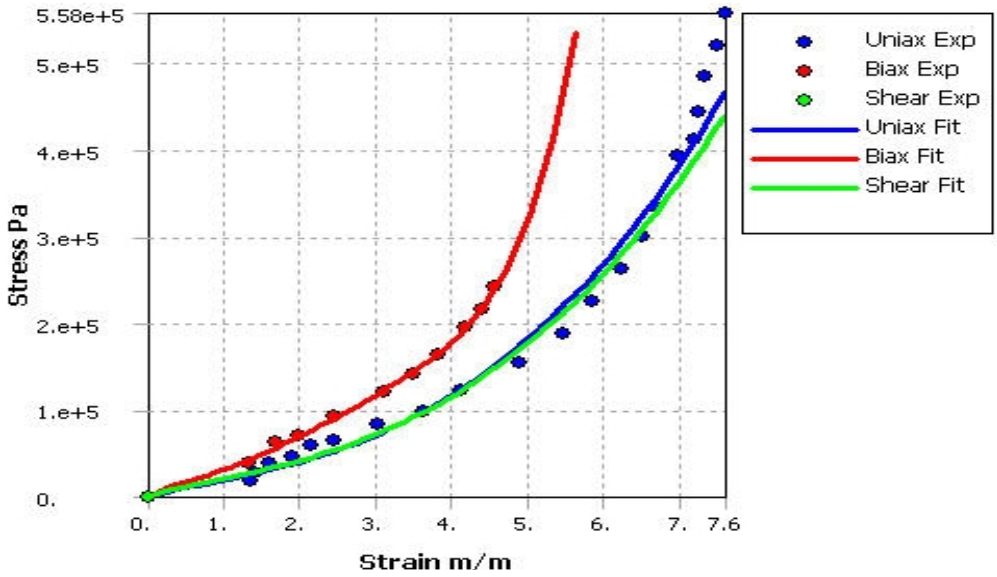

Fig. 4. Mooney-Rivling parameter constitutive equation used within the ANSYS 10 shows very close prediction of the rubber sample behavior. It means that Mooney-Rivling parameter can be safely used for the finite element analysis of the rubber

c) Mesh element design

The mesh element design Fig. 5 was done using the mesh tools built into the ANSYS multiphysis 10. The number of elements is 7442, the number of nodes is 11817 and the depth of refinement is 2. These values were able to give convergence (i.e. solution). Higher values will also work but experience shows for each increase in refinement for example, the processing time increases exponentially.

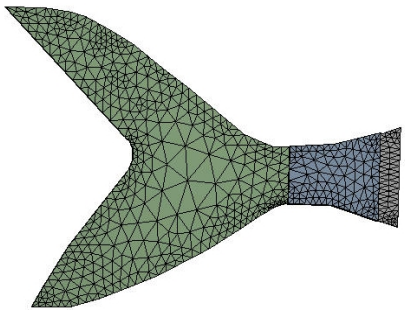

Fig. 5. Optimized ANSYS 10 generated mesh pattern used for the finite element analysis

d) Simulated inputs loads and its derivation for the finite element analysis

The simulated applied loads were based on the following assumptions:

1. The tail section is oscillating at max of 90^o ($+45^o$ to -45^o)
2. It is oscillating at frequency of 1Hz
3. It will operate in water with density of $990kg/m^3$ (sea water)

The loads for simulation are derived as follows;

Angular velocity, $\omega = 2\pi \times 90^o/360^o = ¼ \times 2\pi = ½\pi$ rad/s, that is from $+45^o$ to -45^o

If centroid = r ≈ 20mm, } estimated using Autodesk Inventor 7.
Area of fin = A =0.002427 m^2 }
C_d = 1.28 The tail fin interaction with water will be as a flat plate with area A,
ρ = 990kg/m^3 Water density

Then, the force that will act on the peduncle will be equal to the drag force on the fin, from equation 7;

Drag force, F_d = ½ x 990 x $(0.03142)^2$ x 1.28 x 0.002427 ≈ 0.001N
Perpendicular load across its surface is expected to be the major load
= Drag force, F_d = 0.001N

The simulated loads are shown in Fig. 6.

Furthermore, the glued parts (contacts) are specified to be bonded in the simulation process. Also the large deflection criterion was set on due to the presence of hyper-elastic material (natural rubber) in the composite structure.

2.1.3 The dynamic load experienced by the peduncle

Calculating the dynamic torque uses the same assumption stated in section 2.1.2 (d)
If A= 0.002427 m^2 (tail fin surface area), R≈20mm = approximately centroid from AutoCAD Inventor 7. Maximum oscillating angle = ($+45^o$ to -45^o) = 90^o = π/2, that is angular displacement = π/2 * 2 = π. Also period of oscillation = 1s (that is using simulation

frequency of 1Hz) and thus angular velocity = π * 1 = π rad/s= angular displacement / time to perform the displacement.

Then, linear velocity = angular velocity * r = π rad/s * 0.02m = 0.0628m/s
ω_v = Linear velocity (which is equivalent to the linear velocity in this scenario, [23]).
=0.0628m/s
= Instantaneous velocity of the tail. The minimum is 0m/s (i.e. coasting).

Therefore dynamic pressure = 0.5 * 990 kg/m^3 * (0.0628m/s)^2 from equation 10
$F_v = P_v * A$ = 1.9522 N/m^2 * 0.002427m^2 = 0.00474 N

From Fig. 3, dynamic torque = F_v * r=0.00474 N * 0.02m=0.0000949Nm = torque at the peduncle centroid. This is the torque required for 1Hz tail beat frequency at 90^o angular displacement inside water of density 990kg/m^3. The result and discussion section shows the result for other parameter combinations.

2.1.4 Frequency induced softening of the rubber (PAYNE effect)

This was determined experimentally using a frequency loss machine design presented by Afolayan et al. [27].

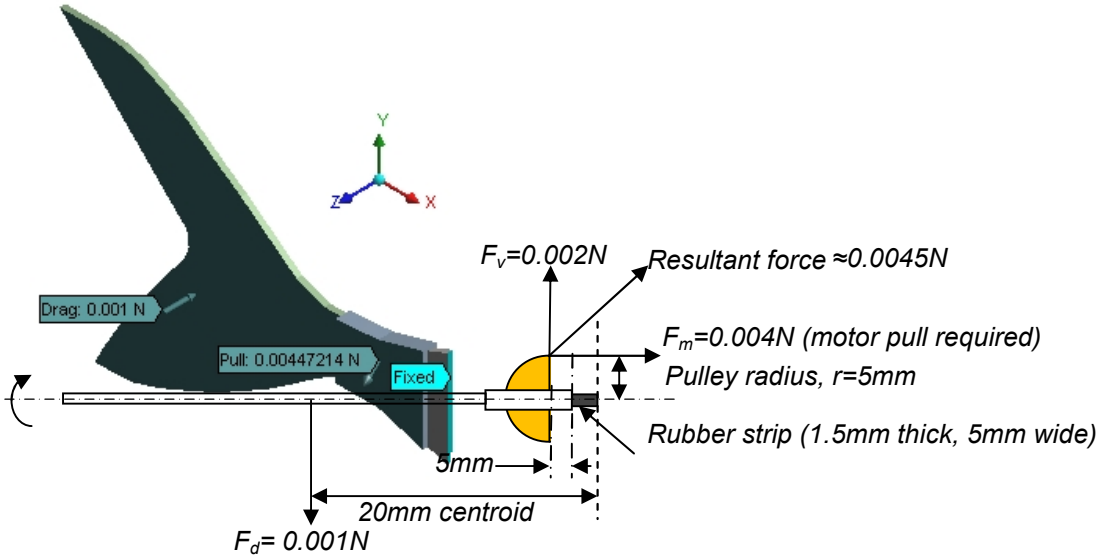

Fig. 6. The simulation inputs: Drag force F_d (0.001N) on the fin and 0.0045N reactive force (vector sum of 0.002N –z axis and 0.004 N - x axis) on the plywood support. F_v and F_m are derived using moment of forces about the edge of the rubber strip

2.1.5 List of items simulated

The simulation was performed specifically to find the range and load distribution experienced by the rubber based joint, the plywood support and the plywood fin when subjected to the calculated virtual loads as presented earlier. Also the possibility of warping of the design was

checked using directional deformation tool built into ANSYS. The behavior of the glue interfaces was also checked using contact analysis tool.

3. RESULTS AND DISCUSSION

3.1 Stress within the Components of the Peduncle

The result of the computer simulation of forces on the surface of the peduncle is shown in Fig. 7 from which the von Mises maximum stress in the rubber is $0.464x10^4$Pa = 4.64kN/m^2 and the minimum is $0.003x10^4$Pa = 0.03kN/m^2. It will also be noted that the higher stress concentration is at the middle (longitudinally) where bending is expected to occur.

For the (plywood) support, the von Mises Maximum stress is $0.924x10^4$Pa = 8.24kN/m^2 occurring at the junction between it and the fin. The minimum von Mises stress is $0.003x10^4$Pa = 0.03kN/m^2 occurring at the junction between it and the rubber joint.

The maximum von Mises stress experienced by the fin is $4.148x10^4$Pa = 41.48kN/m^2 and the minimum is $0.003x10^4$Pa = 0.03kN/m^2. The maximum occurred at the top bend and lower bend just before the support.

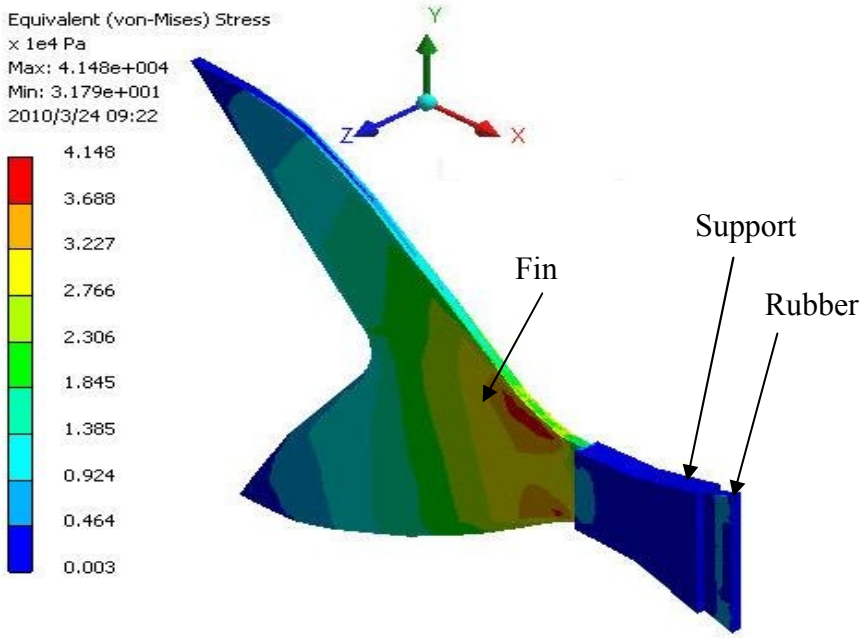

Fig. 7. Simulation Result – von Mises stress acting within the peduncle using the simulated loads

3.2 Stress Experienced by the Peduncle under Its Own Weight

Fig. 8 shows the simulation result of the peduncle under vertical loading or its own weight (i.e. the cantilever effect). For the rubber component, the maximum von Mises stress experienced in the rubber is $4.889x10^3$Pa = 4.9kN/m^2 and the minimum von Mises stress experienced is 0 Pa = 0 kN/m^2. It is interesting to note that the rubber middle marked **A** on

Fig. 8 has zero stress. This implies that that portion will retain its grip with the other portion of the fish robot while the other section marked **B** may be giving way under its own weight. The stress in the plywood support ranges from 0 $x10^3$Pa to 1.087 $x10^3$Pa. The fin itself bears no stress value.

3.3 Test For Warping/ Bending of the Peduncle

The deformation (or warping) simulation result is shown in Fig. 9. The isoline shows straight pattern. A warped assembly will show contoured lines. It can thus be concluded that the assembly will maintain the rigidity required in operation.

3.4 Tensile Stress within the Bonded Joints

The contact analysis result of the simulation is shown in Fig. 10. It was scaled as being sticking, sliding, near and far. The two contacts analyzed shows that both are sticking, that is, the materials will be bonded properly. This implies that the joint will not separate under the peduncle's own weight.

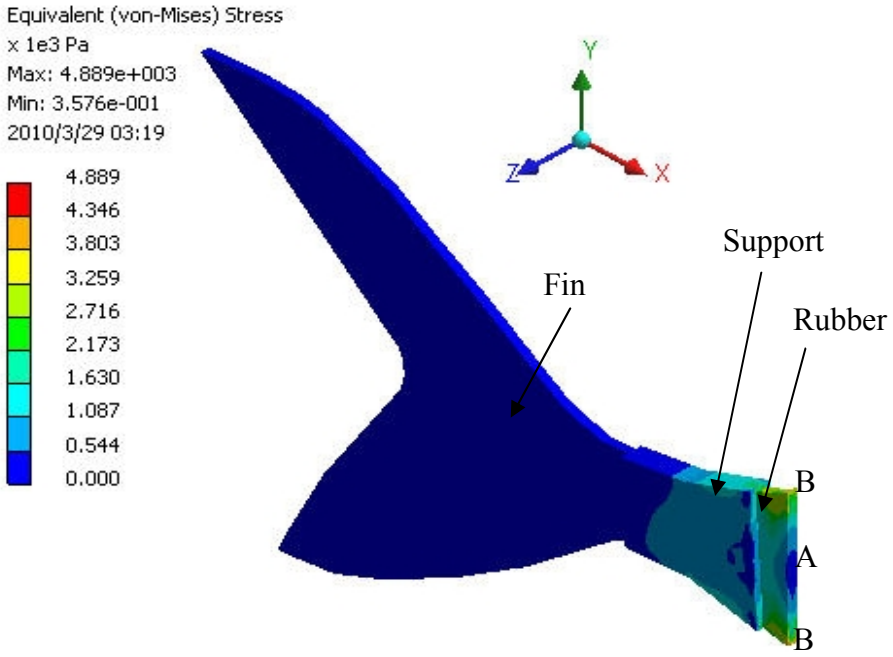

Fig. 8. von Mises stress within the peduncle under its own static weight

3.5 Dynamic Torque experienced by the Peduncle

The Fig. 11 is the graphical representation of the dynamic torque experienced at various angles and various oscillation frequencies of swinging. These data are derived using section 2.1.3 example. The dynamic torque increases with frequency of oscillation and even more rapidly as the angle of swing increases though at a fixed ratio to each other, for example, the dynamic torque at 90deg swing angle is 4 times that of 45deg swing angle and 324 times that at 5deg at all swing angle of oscillation.

3.6 Frequency Induced Softening (Payne Effect)

Fig. 12 shows the lags due to the rubber stiffness at various experimental frequencies used. The frequencies used are 0.5Hz, 1Hz, 5Hz, 10Hz, 15Hz, 20Hz, 25Hz and 30Hz. Three experiments were conducted for each frequency at three stabilized temperatures of a = (33.80 ± 0.01^{o}C), b= (34.89 ± 0.04^{o}C) and c = (34.91 ± 0.01^{o}C).

The rubber becomes soft as the frequency reaches 25Hz. The implication is that the rubber should not be made to oscillate at frequencies beyond 25Hz, otherwise, the rigidity will be lost and the design using that rubber will fail. However, for our robotic fish, the frequency of interest is 0 to 10Hz as indicated in Fig. 12 which is within the safe limit.

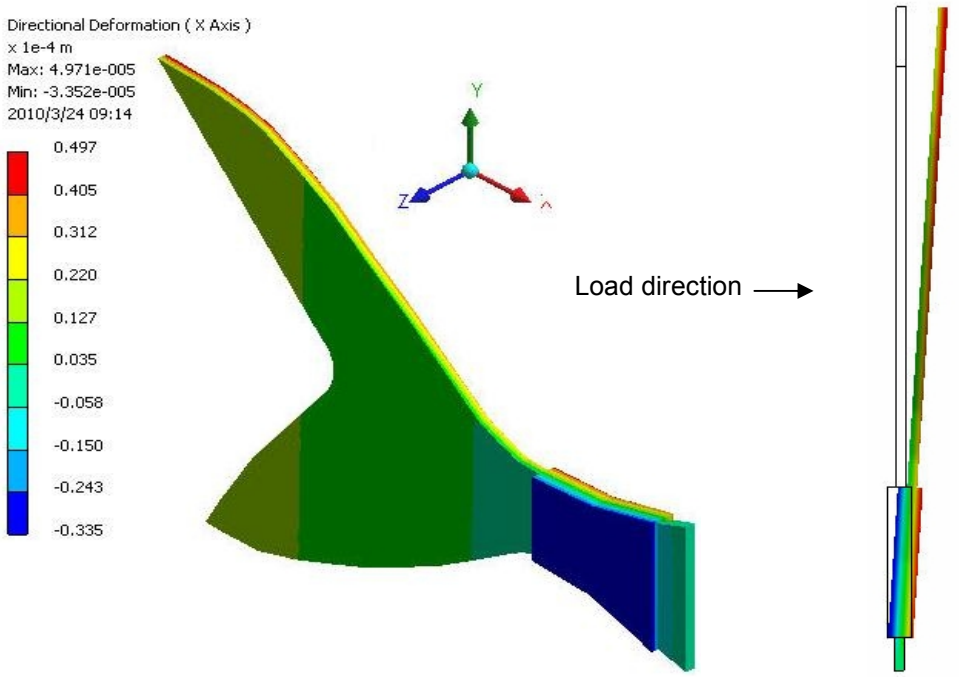

Fig. 9. Simulation Result – Directional deformation – It shows vertical straight patterns. The top view further shows the evidence of rigid non warping bending. The implication of this is that a rigid support is guaranteed for the Hydrostatic skeleton

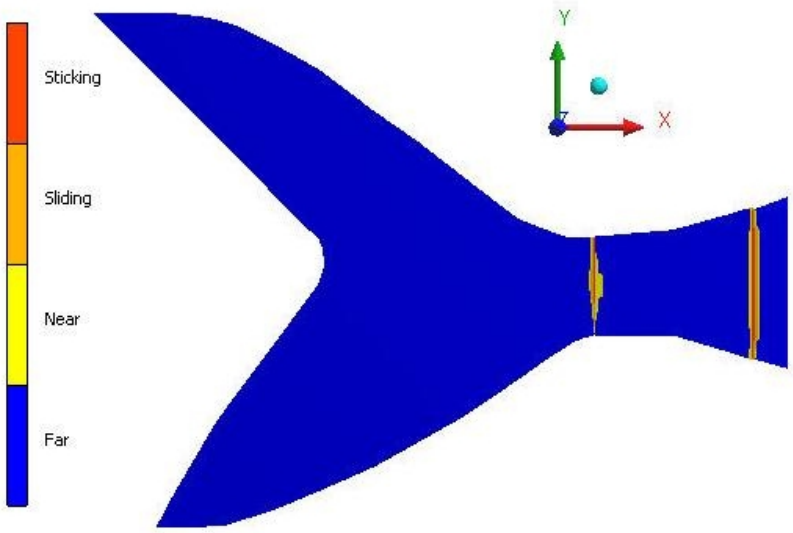

Fig. 10. The contact analysis of the composite material. All the glued contacts shows a complete sticking which implies that the weight and loads will be spread/absorbed properly

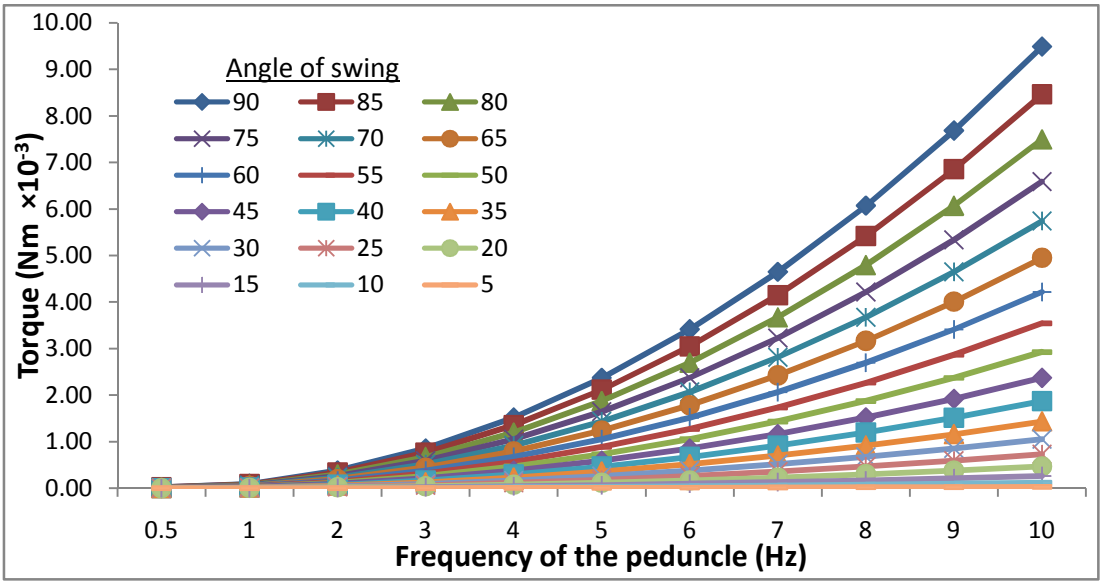

Fig. 11. Dynamic torque developed at different peduncle oscillation frequency and swing angle

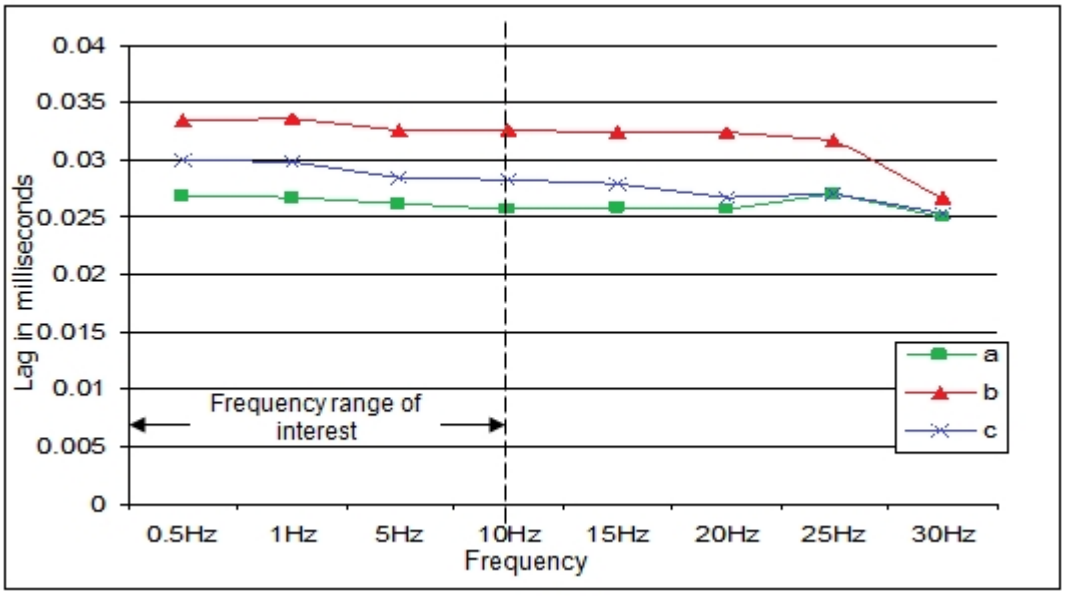

Fig. 12. Frequency response plot of the rubber used for the peduncle joint at environmental temperature of a, b, c.
a = (33.80 ± 0.01°C), b= (34.89 ± 0.04°C) and c = (34.91 ± 0.01°C)

4. CONCLUSION

This work presents a simulation process of the forces and loads (dynamic loads) that this particular design of a robotic fish peduncle will experience. The peduncle uses natural rubber for its flexible joint and simulation has proved that the stress developed can be handled by this rubber material especially if the frequency of oscillation does not exceed 25Hz. Fortunately, the fish tail oscillation does not require frequency above 10Hz, though our robotic fish was able to attain 4.3Hz when not inside water. Also, the use of plywood material for the fin will be adequate also as proofed in the simulation.

ACKNOWLEDGEMENTS

This project was supported by MacArthur Foundation and Ahmadu Bello University Board of Research grant.

COMPETING INTERESTS

This project was supported by MacArthur Foundation and Ahmadu Bello University Board of Research Grant.

REFERENCES

1 Lilianes Peters. Robotics, ERCIM News No. 42, July 2000;8-9. Available: www.ercim.org.
2 Meyer J, Guillot A. Biologically Inspired Robots. In: Bruno S, Oussama K, editors. Handbook of Robotics. Springer (Malestrom); 2008.

3 Zufferey JC, Floreano D. Toward 30-gram Autonomous Indoor Aircraft: Vision-based Obstacle Avoidance and Altitude Control. Proceedings of the 2005 IEEE International Conference on Robotics & Automation Barcelona, Spain. 2005;18-22,

4 Harrison RR, Koch C. A Silicon Implementation of the Fly's Optomotor Control System in Letter by M.V. Srinivasan and Stephen DeWeerth. Neural Computation. Massachusetts institute of Technology. 2000;12:2291-2304.

5 Brett RF, William HW, Selim T, Leslie PK. A dynamic Model of Visually- Guided Steering, Obstacle Avoidance, and Route Selection. International Journal of Computer Vision. 2003;54(1/2/3):13-34.

6 Srinivasan MV. Distance Perception in Insects. Centre for Visual Sciences, Research School of Biological Sciences, Australian National University. Published by Cambridge University Press; 1992.

7 Srinivasan MV, Zhang SW, Chahl JS, Stange G, Garratt M. An overview of insect-inspired guidance for application in ground and airborne platforms. Proc. Instn Mech Engrs Vol 218 Part G: J Aerospace Engineering. 2004;375-388.

8 Park SJ, Goodman MB, Pruitt BL. Analysis of nematode mechanics by piezoresistive displacement clamp. PNAS. October 30, 2007;104(44).

9 The Honda ASIMO Robot. Accessed 19 June 2013. Available: http://world.honda.com/ASIMO/.

10 Available:http://www.sony.net/SonyInfo/News/Press_Archive/199905/99-046/ Accessed 19 June 2013.

11 Grasso FW. Flow- and Chemo-sense for Robot and Lobster Guidance in Odor Source Tracking. Neurotechnology for Biomimetic Robots Conference. May-14-16, 2000 at Northeastern University East Point, Nahant, MA 01908

12 Robots That Can Taste. Accessed 19 June 2013. Available: http://www.robotorama.com/archives/2008/03/06/robots-that-can-taste/

13 Yamada H, Chigisaki S, Mori M, Takita K, Ogami K, Hirose S. Development of Amphibious Snake-like Robot ACM-R5, ISR2005, Proc. ISR. 2005;133.

14 William C. Snake-Like Robot Can Crawl on Land or Swim. Accessed 1 June 2013. Available:http://www.gorobotics.net/The-News/Latest-News/Snake%11Like-Snake-Like-Robot-Can-Crawl-on-Land-or-Swim/

15 Yamada H, Hirose S. Development of Practical 3-Dimentinal Active Cord Mechanism ACM-R4. Journal of Robotics and Mechatronics. 2006;18(3):305-311.

16 Kevin JD. Limbless Locomotion: Learning to Crawl with a Snake Robot. A PhD thesis at the Robotics Institute Carnegie Mellon University, 5000 Forbes Avenue, Pittsburg, PA 15213.

17 Shugen MA, Mitsuru Watanabe. Time-optimal control of kinematically redundant manipulators with limit heat characteristics of actuators. Advanced Robotics. 2002;16(8):735-749.

18 Dorfmann A, Trimmer BA, Woods Jr WA. A constitutive Model for Muscle properties in Soft-bodied Arthropod. J. Roy. Soc. Int. 2007;4:257-269.

19 Swimming Speeds of Some Common Fish. Accessed 19 June 2013. Available: http://www.nmri.go.jp/eng/khirata/fish/general/speed/speede.htm.

20 Trimmer BA, Takesian AE, Sweet BM, Rogers CB, Hake DC and Rogers DJ. Caterpillar Locomotion and Burrowing Robots. 7th International Symposium on Technology and Mine Problem, Monterey, CA. 2006;1-10.

21 Ryder GH. Strength of Materials, 3rd Edition. ELBS McGraw-Hill; 1990.

22 Kelly B. Strength/Mechanics of Materials. Accessed 1 June 2013. Available online at: http://www.engineersedge.com/strength_of_materials.htm

23 John JV. Fish Swimming. Chapman and Hall, 2-6 Boundary Row, London SE1 8HN, UK; 1993.

24 Roy B. The theory of adhesive bonding. Accessed 1 August 2011. Available: http://www.roymech.co.uk/Useful_Tables/Adhesives/Adhesive_Bond.html.
25 Lighthill MJ. Large-amplitude elongated-body motion theory. Proceeding of Royal Society. London. Abstract and introduction only. 1971;179:125-138.
26 Beatty MF. The Mullins Effect in the Vibration of Stretched Rubber Membrane. Mathematics and Mechanics of Solids. 2002;8:435-445.
27 Afolayan MO, Yawas DS, Folayan CO, Aku SY. Mechanical Performance of Polyisoprene used in Building a Flapping Foil Underwater Robot. Research Journal of Applied Sciences. Engineering and Technology. 2011;3(6):474-485.

Peer-review history:
The peer review history for this paper can be accessed here:
http://www.sciencedomain.org/review-history.php?iid=226&id=5&aid=2041